

DOI: 10.1002/ange.200500261

# Mimicking the Function of Eggshell Matrix Proteins: The Role of Multiplets of Charged Amino Acid Residues and Self-Assembly of Peptides in Biom mineralization\*\*

Parayil Kumaran Ajikumar,  
Subramanian Vivekanandan,  
Rajamani Lakshminarayanan, Seetharama D. S. Jois,  
R. Manjunatha Kini, and Suresh Valiyaveetil\*

The molecular-level understanding and rationalization of nature's clues on how to produce complex, organized structures such as bone, teeth, and seashells at ambient temperature and in aqueous environments has resulted in the design and synthesis of novel materials.<sup>[1,2]</sup> The properties of the crystals such as size, shape, stability, polymorph selectivity, and crystallographic orientation are controlled by biomacromolecules, which are classified as "framework macromolecules" and "control macromolecules".<sup>[2,3]</sup> The complexities of the natural biom mineralization process have resulted in research efforts being focused on "tailor-made" low-molecular-weight compounds and macromolecular additives for structure–function investigations by in vitro mineralization experiments.<sup>[4]</sup> So far, research efforts have been focused on auxiliary oligopeptides to probe the role of functional motifs in the kinetics, habit modifications, and polymorph selectivity during the crystal growth process.<sup>[5,6]</sup>

The structure–function sequence analysis of eggshell-specific proteins revealed that the presence of multiplets of charged amino acid residues and characteristic self-aggregation in solution influence the formation of biom minerals.<sup>[7,8]</sup> We anticipate that the design and testing of peptides with multiplets of charged residues could mimic the functions of

such proteins during in vitro experiments.<sup>[6c]</sup> Thus, to investigate the role of self-assembly and multiplets of charged amino acids in calcium carbonate mineralization, we designed a series of peptides (Table 1) and studied their structure–activity relationships. The first two groups (I, II) of peptides have an ordered arrangement of doublets of charged residues which resembles the primary structure of avian eggshell matrix proteins (a full sequence comparison is given in the Supporting Information).<sup>[7]</sup> The significant structural differences between the peptides involve replacing the arginine residue with lysine—a basic flexible residue with a primary amino group and hydrophobic side chain—and the incorporation of a proline residue in the middle of the peptides in group II. The proline residue is expected to limit the conformational flexibility,<sup>[6c]</sup> and organisms use such domains to form three-dimensional supramolecular structures of proteins.<sup>[2a,8,9]</sup> Among the three peptides in group III, K<sub>2</sub>E<sub>2</sub>W<sub>2</sub>D<sub>2</sub>G-17 and K<sub>2</sub>AE<sub>2</sub>AW<sub>2</sub>AD<sub>2</sub>P-23 have an ordered arrangement of doublets of charged residues. However, the incorporation of one glycine residue in the former and six alanine residues in the latter peptide is expected to disrupt the ordered, stable secondary structure of the peptides and impart flexibility to the peptide backbone. The peptide (KE)<sub>2</sub>(WD)<sub>2</sub>-16, with alternate acidic and basic residues, is designed as a control peptide for confirming the perceived critical role of multiplets of charged residues.

To understand the role of these designed peptides in calcite growth and habit modification, we carried out in vitro mineralization of calcium carbonate by slow diffusion of CO<sub>2</sub> and NH<sub>3</sub> gas to the peptide dissolved in CaCl<sub>2</sub> solution (7.5 mM).<sup>[10]</sup> The first two groups of peptides showed significant influence on the calcite crystal morphology and aggregation as compared with the group III peptides (compare images 2–5 with images 6–8 in Figure 1 and Supporting Information).

The CaCO<sub>3</sub> crystals formed in presence of group I and II peptides showed—similarly to those formed in the presence of ansocalcin<sup>[8]</sup>—concentration-dependent changes in crystal morphology (Figure 1 and Supporting Information). Polycrystalline aggregates of calcite crystals were formed as the concentration was increased to 2 mg mL<sup>−1</sup>, and the size of the crystal aggregates obtained with K<sub>2</sub>E<sub>2</sub>W<sub>2</sub>D<sub>2</sub>-16 (≈ 41 μm) and K<sub>2</sub>E<sub>2</sub>W<sub>2</sub>D<sub>2</sub>P-17 (≈ 35 μm) was almost double that of crystals obtained with R<sub>2</sub>E<sub>2</sub>W<sub>2</sub>D<sub>2</sub>-16 (≈ 20 μm) and R<sub>2</sub>E<sub>2</sub>W<sub>2</sub>D<sub>2</sub>P-17 (≈ 21 μm). The observed superstructures are composed of smaller rudimentary calcite crystals assembled into spherical structures. The crystal lattice was further characterized by X-ray diffraction studies. In addition, the nucleation density (that is, the number of crystals per unit area) also increased with an increase in the peptide concentration. Group III peptides did not show significant influence on the calcite crystal nucleation, growth, or morphology. This finding indicates that not only the primary structural characteristics but also control of the spatial disposition of the functional sites on the peptide is important for the nucleation of crystal aggregates. Thus, the designed peptides R<sub>2</sub>E<sub>2</sub>W<sub>2</sub>D<sub>2</sub>-16, R<sub>2</sub>E<sub>2</sub>W<sub>2</sub>D<sub>2</sub>P-17, K<sub>2</sub>E<sub>2</sub>W<sub>2</sub>D<sub>2</sub>-16, and K<sub>2</sub>E<sub>2</sub>W<sub>2</sub>D<sub>2</sub>P-17 (2 mg mL<sup>−1</sup>, ≈ 0.8 μm) induce the nucleation and formation

[\*] Dr. P. K. Ajikumar, Dr. R. Lakshminarayanan, Prof. S. Valiyaveetil  
Department of Chemistry and Singapore–MIT Alliance  
National University of Singapore  
3 Science Drive 3, Singapore 117543 (Singapore)  
Fax: (+65) 6779-1669  
E-mail: chmsv@nus.edu.sg

Dr. S. D. S. Jois  
Department of Pharmacy  
National University of Singapore  
Singapore 117543 (Singapore)

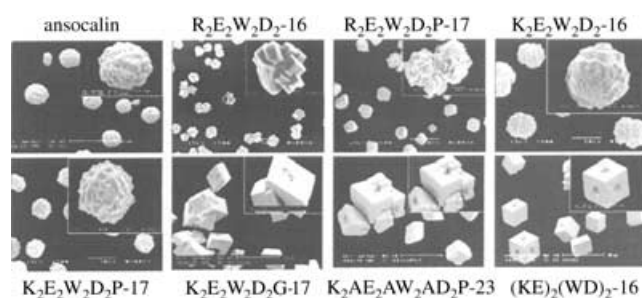
Dr. S. Vivekanandan, Prof. R. M. Kini  
Department of Biological Sciences  
National University of Singapore  
Singapore 117543 (Singapore)

[\*\*] This work was supported by the Singapore–MIT Alliance. R.L. acknowledges Singapore Millennium Foundation for the award of a fellowship. The authors acknowledge technical support from the Departments of Chemistry, Biological Sciences, and Materials Sciences at National University of Singapore.

Supporting information for this article is available on the WWW under <http://www.angewandte.org> or from the author.

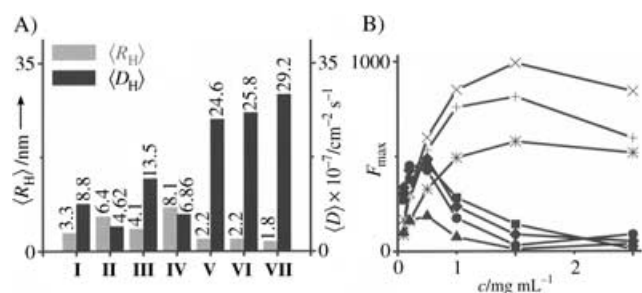
**Table 1:** Details of the amino acid sequences and structure–activity relationships of the model peptides.

Group	Model peptide	Primary structure	Secondary structure	Results Activity in crystal growth
I	R <sub>2</sub> E <sub>2</sub> W <sub>2</sub> D <sub>2</sub> -16 (I)	RREEWDDRRREEWDD	β sheet	polycrystalline calcite aggregate formation
	K <sub>2</sub> E <sub>2</sub> W <sub>2</sub> D <sub>2</sub> -16 (III)	KKEEWDDKKEEWDD	β sheet	
II	R <sub>2</sub> E <sub>2</sub> W <sub>2</sub> D <sub>2</sub> P-17 (II)	RREEWDDPRREEWDD	β sheet with turn	no influence on calcite growth or habit modification
	K <sub>2</sub> E <sub>2</sub> W <sub>2</sub> D <sub>2</sub> P-17 (IV)	KKEEWDDPKKEEWDD	β sheet with turn	
III	K <sub>2</sub> E <sub>2</sub> W <sub>2</sub> D <sub>2</sub> G-17 (V)	KKEEWDDGKKEEWDD	unordered	
	K <sub>2</sub> AE <sub>2</sub> AW <sub>2</sub> AD <sub>2</sub> P-23 (VI)	KKAEAAWADDPKAEAAWADD		
	(KE) <sub>2</sub> (WD) <sub>2</sub> -16 (VII)	KEKEWDWDKEKEWDWD		


**Figure 1.** Crystal habit modification in the presence of the protein ansocalcin (500 μg mL<sup>-1</sup>) and designed peptides (2 mg mL<sup>-1</sup>). The scale bars represent 50 μm. Magnified images are given in the insets.

of polycrystalline calcite crystal aggregates similar to the parent protein ansocalcin.

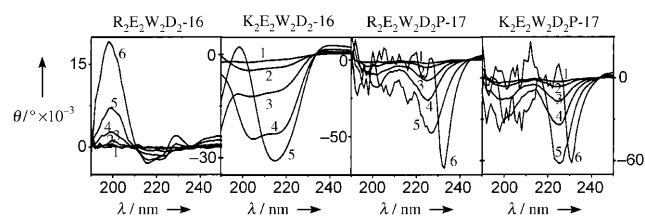
For a detailed investigation of the structure–activity relationship, we investigated the self-assembly of the peptides in solution by dynamic light scattering (DLS), tryptophan fluorescence, circular dichroism (CD), NMR spectroscopy, and molecular modeling studies. The DLS and fluorescence analysis showed a concentration-dependent aggregation of group I and II peptides in CaCl<sub>2</sub> solution (Figure 2). The observed hydrodynamic radii of the group I peptides ( $\langle R_H \rangle = 3.3$  and 4.1 nm) are smaller than those of the corresponding proline-incorporated group II peptides ( $\langle R_H \rangle = 6.4$  and 8.1 nm). However, a fourfold reduction in the size of the aggregate was observed when proline in K<sub>2</sub>E<sub>2</sub>W<sub>2</sub>D<sub>2</sub>P-17 (IV, 8.1 nm) was replaced with glycine in K<sub>2</sub>E<sub>2</sub>W<sub>2</sub>D<sub>2</sub>G-17 (V, 2.2 nm). These results highlight the expected role of proline


**Figure 2.** A) Mean hydrodynamic radius ( $\langle R_H \rangle$ ) and diffusion coefficient ( $\langle D \rangle$ ) of synthetic peptides I–VII. The y axis represents the  $\langle R_H \rangle$  in nanometers or  $\langle D \rangle \times 10^{-7}$  in cm<sup>2</sup> s<sup>-1</sup>. B) Intensity ( $F_{\max}$ ) versus concentration profile of fluorescence emission of synthetic peptides I (●), II (■), III (▲), IV (●), V (▲), VI (+), and VII (×) in CaCl<sub>2</sub> solution (7.5 mM).

toward decreasing the conformational flexibility and enhancing the oligomerization of peptides into large aggregates. The observed particle sizes for the group III peptides K<sub>2</sub>AE<sub>2</sub>AW<sub>2</sub>AD<sub>2</sub>P-23 (VI, 2.2 nm) and (KE)<sub>2</sub>(WD)<sub>2</sub>-16 (VII, 1.8 nm) were low. Interestingly, alterations of the peptide sequences result in the enhancement of the mean diffusion coefficient ( $\langle D \rangle$ , Figure 2). In addition, the observed mean diffusion coefficient for the group I and II peptides is almost comparable to that of monomeric forms of ansocalcin and lithostathine.<sup>[8,11]</sup>

The study of the microenvironment around the tryptophan residues gives an insight into the self-aggregation tendency of the peptides. All the peptides showed distinct emission characteristics (see Supporting Information) and changes in intensity of the emission maximum with change in peptide concentration. The lysine-incorporated peptides K<sub>2</sub>E<sub>2</sub>W<sub>2</sub>D<sub>2</sub>-16 and K<sub>2</sub>E<sub>2</sub>W<sub>2</sub>D<sub>2</sub>P-17 showed weaker emission intensities than the peptides R<sub>2</sub>E<sub>2</sub>W<sub>2</sub>D<sub>2</sub>-16 and R<sub>2</sub>E<sub>2</sub>W<sub>2</sub>D<sub>2</sub>P-17. Notably, the intensity increased linearly with concentration up to 0.25 mg mL<sup>-1</sup>, followed by an approximately 85 % decrease in intensity for groups I and II peptides at a concentration of 2 mg mL<sup>-1</sup>. This result might be a consequence of the quenching of the tryptophan fluorescence by the polar functional groups (CO<sub>2</sub>H), which are brought into close proximity through aggregation of the peptide molecules.<sup>[12]</sup> However, in the case of the group III peptides, the emission intensity increased linearly with concentration up to 1 mg mL<sup>-1</sup> followed by a small intensity drop at 2 mg mL<sup>-1</sup>.

The CD spectra of the peptides were recorded in a concentration range of 0.05 to 2 mg mL<sup>-1</sup> at 25 °C in CaCl<sub>2</sub> solution (Figure 3 and Supporting Information). It is clear that the secondary structure of the peptides R<sub>2</sub>E<sub>2</sub>W<sub>2</sub>D<sub>2</sub>-16 and K<sub>2</sub>E<sub>2</sub>W<sub>2</sub>D<sub>2</sub>-16 in solution is an extended β-sheet conformation


**Figure 3.** Circular dichroism spectra of group I and II peptides in CaCl<sub>2</sub> (7.5 mM) at various concentrations: 1) 50 μg mL<sup>-1</sup>, 2) 100 μg mL<sup>-1</sup>, 3) 250 μg mL<sup>-1</sup>, 4) 500 μg mL<sup>-1</sup>, 5) 1 mg mL<sup>-1</sup>, and 6) 2 mg mL<sup>-1</sup>. The instrument settings used were: scan range, 190 to 260 nm; scan rate, 50 nm min<sup>-1</sup>; sensitivity, 10 millidegrees; response time, 1 s.

at high peptide concentrations ( $2 \text{ mg mL}^{-1}$ ). However, the incorporation of the proline in the middle of the sequences ( $\text{R}_2\text{E}_2\text{W}_2\text{D}_2\text{P-17}$  and  $\text{K}_2\text{E}_2\text{W}_2\text{D}_2\text{P-17}$ ) disrupts the extended  $\beta$ -sheet structure. The CD spectra showed the appearance of an amide  $n\text{--}\pi^*$  negative-transition band at 225 and 227 nm for the peptides, which corresponds to a  $\beta$ -turn conformation.<sup>[13]</sup> The replacement of proline with glycine in  $\text{K}_2\text{E}_2\text{W}_2\text{D}_2\text{G-17}$  resulted in an unordered structure with turns (negative minimum at 201 and 223 nm).<sup>[14]</sup> Similarly, the CD spectra of the peptides  $\text{K}_2\text{AE}_2\text{AW}_2\text{AD}_2\text{P-23}$  (negative minimum at 199 and 224 nm) and  $(\text{KE})_2(\text{WD})_2\text{-16}$  (negative minimum at 199 nm and a weak positive maximum at 216 nm) also indicated unordered structures in solution.

The results obtained from CD spectrometry are supported by data from NMR experiments. The 1D NMR spectra of  $\text{R}_2\text{E}_2\text{W}_2\text{D}_2\text{-16}$  and  $\text{K}_2\text{E}_2\text{W}_2\text{D}_2\text{-16}$  showed a significant peak broadening (Figure 4A) as a result of the formation of an

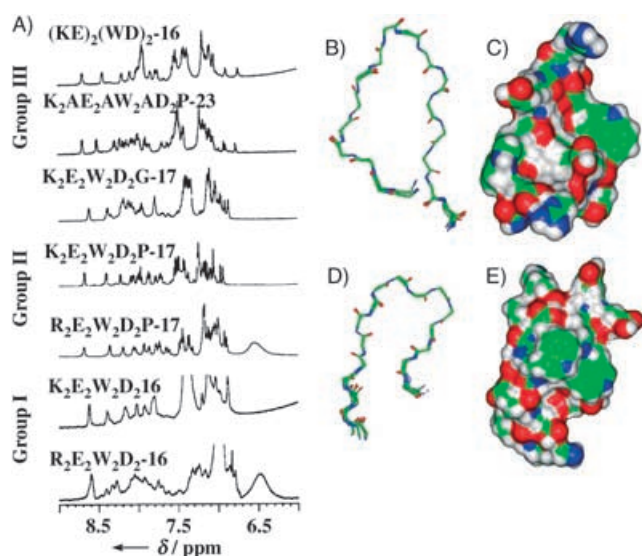


**Figure 4.** A) 1D pulsed-field gradient  $^1\text{H}$  NMR spectra of the NH region of the model peptides; 300 K, in 90%  $\text{H}_2\text{O}$ /10%  $\text{D}_2\text{O}$ , pH 3.0. Proton chemical shifts are referenced from internal  $[2,2,3,3\text{-D}_4]\text{TSP}$ . B)–E) Conformational ensembles and surface structures obtained from molecular dynamics simulations of the peptides  $\text{R}_2\text{E}_2\text{W}_2\text{D}_2\text{P-17}$  (B, C) and  $\text{K}_2\text{E}_2\text{W}_2\text{D}_2\text{P-17}$  (D, E).

extended  $\beta$ -sheet conformation in solution. In contrast, the 1D NMR spectra of the peptides  $\text{R}_2\text{E}_2\text{W}_2\text{D}_2\text{P-17}$  and  $\text{K}_2\text{E}_2\text{W}_2\text{D}_2\text{P-17}$  showed sharp NH peaks within the range of  $\Delta\delta = 1.3 \text{ ppm}$ , which indicates an ordered structure in solution. The NMR spectrum of  $\text{K}_2\text{E}_2\text{W}_2\text{D}_2\text{G-17}$  showed a strong overlap of amide protons, thus indicating an unordered structure. Similarly, the peptides  $(\text{KE})_2(\text{WD})_2\text{-16}$  and  $\text{K}_2\text{AE}_2\text{AW}_2\text{AD}_2\text{P-23}$  also showed an extensive chemical shift overlap, which indicated an unordered structure in solution. The calculated proton chemical shift difference measured with TSP references ( $\text{TSP} = 3\text{-(trimethylsilyl)propionate}$ ) showed deviation from the random coil values for the  $\text{R}_2\text{E}_2\text{W}_2\text{D}_2\text{P-17}$  and  $\text{K}_2\text{E}_2\text{W}_2\text{D}_2\text{P-17}$  peptides (see Supporting Information).<sup>[15]</sup>

The calculated  $\delta$  values for residues E4–D7 and R/K10–D17 in the group II peptides are greater than random coil values by 0.1 ppm, which indicates that both peptides adopt a similar nonextended conformation with a turn structure for the backbone. The calculated ratio of  $d_{\text{aN}}(i,i+1):d_{\text{NN}}(i,i+1)$  is greater than 1.4, which suggests an ordered peptide conformation. A long-range NOE cross-relaxation transfer ( $d_{\text{aN}}(i,i+2)$ ) was observed between the residues P9/R11 and E12/W14 for  $\text{R}_2\text{E}_2\text{W}_2\text{D}_2\text{P-17}$  and D8/K10, P9/K11, and E12/W14 for  $\text{K}_2\text{E}_2\text{W}_2\text{D}_2\text{P-17}$  (see Supporting Information). However, in the case of the glycine-containing peptide ( $\text{K}_2\text{E}_2\text{W}_2\text{D}_2\text{G-17}$ ), no  $d_{\text{NN}}(i,i+1)$  NOE connectivities were observed. Thus, from the above observations we conclude that the peptides  $\text{R}_2\text{E}_2\text{W}_2\text{D}_2\text{P-17}$  and  $\text{K}_2\text{E}_2\text{W}_2\text{D}_2\text{P-17}$  adopt a nonextended structure with a turn or kink on the backbone.

By using the available NMR restraints, the conformations of the peptides were calculated with the help of molecular-dynamics-simulated annealing/minimization experiments to determine a plausible lowest-energy conformational ensemble (ten structures) that fits the target NMR data set. The conformers with the fewest NOE violations were used to represent the structure. Figures 4B, D show the backbones of ten overlapped, energy-minimized structures of the peptides  $\text{R}_2\text{E}_2\text{W}_2\text{D}_2\text{P-17}$  and  $\text{K}_2\text{E}_2\text{W}_2\text{D}_2\text{P-17}$ , whereas the surface structures (Figure 4C, E) represent the distribution of functional groups. Analysis of the  $\phi, \psi$  distribution obtained for the ten conformational ensembles revealed that the dihedral pairs near proline consistently centered within the  $\phi, \psi$  regions associated with a turn structure in polypeptides. Comparison of the dihedral angles shows a type II turn structure near P9–R10 residues of the peptide  $\text{R}_2\text{E}_2\text{W}_2\text{D}_2\text{P-17}$  and a type I turn structure in the region of P9–R10 and E12 to E13 of  $\text{K}_2\text{E}_2\text{W}_2\text{D}_2\text{P-17}$ .

The observations from the CD and NMR spectra and molecular modeling studies are well-correlated and consistent. The peptides  $\text{R}_2\text{E}_2\text{W}_2\text{D}_2\text{P-17}$  and  $\text{K}_2\text{E}_2\text{W}_2\text{D}_2\text{P-17}$  exhibit a  $\beta$ -sheet-type structure with a turn near the proline residue. Such an unfolded conformation would minimize the electrostatic side-chain charge repulsion, orient the charged residues (D, E, R, and K), and make them accessible for complexation with calcium ions in solution.<sup>[16]</sup>

The observed extensive overlap of the NMR signals in the amide region of group III peptides indicates the presence of an unordered open structure with rapid conformational exchanges. In addition, the low hydrodynamic radius ( $\langle R_{\text{H}} \rangle$ ) and high value of the mean diffusion coefficient ( $\langle D \rangle$ ) obtained from the DLS experiments also corroborate the findings from the CD and NMR studies. Moreover, the fluorescence studies revealed the absence of concentration-dependent self-assembly of group III peptides in solution. The results from conformational studies of the peptides are consistent with the observed mineralization behavior in solution. Thus, in the nonaggregated form, the random movement of the peptides resulted in a nonspecific interaction with the  $\text{CaCO}_3$  crystals, thereby inducing pits and truncation of the calcite crystal surfaces.

In conclusion, seven peptides were designed and fully characterized to mimic the function of the goose eggshell matrix protein, ansocalcin. The ordered arrangement of



doublets of charged residues and the self-assembling characteristics of the group I and II peptides generated a functional-group-segregated surface which facilitates the nucleation, growth, and aggregation of calcium carbonate crystal nuclei to form polycrystalline calcite crystal aggregates. The group III peptides showed an unordered structure in solution and no activity toward mineralization. This finding is supported by evidence from DLS, NMR, CD, and fluorescence spectroscopy investigations.

Received: January 24, 2005

Revised: May 5, 2005

Published online: August 1, 2005

**Keywords:** biomineralization · eggshell · peptides · proteins · structure–activity relationships

- [1] a) *Materials Synthesis Based on Biological Processes* (Eds.: M. Alper, P. D. Calvert, R. Frankel, P. C. Rieke, D. A. Tirrell), Materials Research Society, Pittsburgh, PA, **1991**; b) *Biomimetic Materials Chemistry* (Ed.: S. Mann), VCH, New York, **1996**; c) S. Zhang, *Nat. Biotechnol.* **2003**, *21*, 1171–1178.
- [2] a) H. A. Lowenstam, S. Weiner, *On Biomineralization*, Oxford University Press, New York, **1989**; b) S. Mann, *Biomineralization: Principles and Concepts in Bioinorganic Materials Chemistry*, Oxford University Press, New York, **2001**.
- [3] a) C. M. Zaremba, A. M. Belcher, M. Fritz, Y. L. Li, S. Mann, P. K. Hansma, D. E. Morse, J. S. Speck, G. D. Stucky, *Chem. Mater.* **1996**, *8*, 679–690; b) H. C. Lichtenegger, T. Schoberl, M. H. Bartl, H. Waite, G. D. Stucky, *Science* **2002**, *298*, 389–392; c) L. Addadi, S. Weiner, *Angew. Chem.* **1992**, *104*, 159–176; *Angew. Chem. Int. Ed. Engl.* **1992**, *31*, 153–169.
- [4] a) A. P. Wheeler, C. S. Sikes in *Chemical Aspects of Regulation of Mineralization* (Eds.: C. S. Sikes, A. P. Wheeler), University of South Alabama, Mobile, AL, **1988**, pp. 9–13; b) A. P. Wheeler, C. S. Sikes in *Material Synthesis Utilizing Biological Process* (Eds.: P. C. Rieke, P. D. Calvert, M. Alper), Materials Research Society, Pittsburgh, PA, **1989**, pp. 45–50; c) S. Mann, D. D. Archibald, J. M. Didymus, T. Douglas, B. R. Heywood, F. C. Meldrum, N. J. Reeves, *Science* **1993**, *261*, 1286–1292; d) J. M. Didymus, P. Oliver, S. Mann, A. L. Devries, P. V. Hauschka, P. Westbroek, *J. Chem. Soc. Faraday Trans.* **1993**, *89*, 2891–2900; e) A. Wierzbicki, C. S. Sikes, J. D. Madura, B. Drake, *Calcif. Tissue Int.* **1994**, *54*, 133–141; f) C. Geffroy, A. Foissy, J. Persello, B. Cabane, *J. Colloid Interface Sci.* **1999**, *211*, 45–53; g) D. K. Keum, K.-M. Kim, K. Naka, Y. Chujo, *J. Mater. Chem.* **2002**, *12*, 2449–2452; h) K. Naka, *Top. Curr. Chem.* **2003**, *228*, 141–158.
- [5] a) Y. Levi, S. Albeck, A. Brack, S. Weiner, L. Addadi, *Chem. Eur. J.* **1998**, *4*, 389–396; b) S. R. Whaley, D. S. English, E. L. Hu, P. F. Barbara, A. M. Belcher, *Nature* **2000**, *405*, 665–668; c) C. Li, G. D. Botsaris, D. L. Kaplan, *Cryst. Growth Des.* **2002**, *2*, 387–393; d) M. Gilbert, J. W. Shaw, J. R. Long, K. Nelson, G. P. Drobny, C. M. Giachelli, P. S. Stayton, *J. Biol. Chem.* **2000**, *275*, 16213–16218; e) B. Zhang, B. A. Wustman, D. E. Morse, J. S. Evans, *Biopolymers* **2002**, *63*, 358–372; f) B. Zhang, G. Z. Xu, J. S. Evans, *Biopolymers* **2000**, *54*, 464–475; g) B. A. Wustman, D. E. Morse, J. S. Evans, *Langmuir* **2002**, *18*, 9901–9906; h) B. A. Wustman, J. C. Weaver, D. E. Morse, J. S. Evans, *Connect. Tissue Res.* **2003**, *44*, 10–15; i) G. He, T. Dahl, A. Veis, A. George, *Nat. Mater.* **2003**, *2*, 552–558.
- [6] a) D. B. DeOliveria, R. A. Laursen, *J. Am. Chem. Soc.* **1997**, *119*, 10627–10631; b) D. J. H. Gaskin, K. Starck, E. N. Vulfson, *Biotechnol. Lett.* **2000**, *22*, 1211–1216; c) P. K. Ajikumar, R. Lakshminarayanan, S. Valiyaveetil, R. M. Kini, *Biomacromolecules* **2003**, *4*, 1321–1326; d) D. Volkmer, M. Fricke, T. Huber, N. Sewald, *Chem. Commun.* **2004**, 1872–1873.
- [7] a) R. Lakshminarayanan, S. Valiyaveetil, R. M. Kini, *Proc. Natl. Acad. Sci. USA* **2002**, *99*, 5155–5159; b) R. Lakshminarayanan, S. Valiyaveetil, V. S. Rao, R. M. Kini, *J. Biol. Chem.* **2003**, *278*, 2938–2946; c) R. Lakshminarayanan, J. S. Joseph, S. Valiyaveetil, R. M. Kini, *Biomacromolecules* **2005**, *6*, 741–751.
- [8] a) K. Mann, F. Siedler, *Biochim. Biophys. Acta Proteins Proteom.* **2004**, *1696*, 41–50; b) J. P. Reyes-Grajeda, A. Moreno, A. Romero, *J. Biol. Chem.* **2004**, *279*, 40876–40881; c) K. Mann, *Br. Poult. Sci.* **2004**, *45*, 483–490.
- [9] a) M. Bergdoll, M. H. Remy, C. Cagnon, J. M. Masson, P. Dumas, *Structure* **1997**, *5*, 391–398; b) M. W. MacArthur, J. M. Thornton, *J. Mol. Biol.* **1991**, *218*, 397–412; c) S. C. Benson, F. H. Wilt in *Calcification in Biological Systems* (Ed.: E. Bonucci), CRC, Boca Raton, FL, **1992**, pp. 157–178; d) J. P. Gorski, *Calcif. Tissue Int.* **1992**, *50*, 391–396; e) J. Moradian-Oldak, J. Tan, A. G. Fincham, *Biopolymers* **1998**, *46*, 225–238; f) J. Moradian-Oldak, W. Leung, A. G. Fincham, *J. Struct. Biol.* **1998**, *122*, 320–327; g) C. E. Killian, F. C. Wilt, *J. Biol. Chem.* **1996**, *271*, 9150–9159.
- [10] S. Albeck, J. Aizenberg, L. Addadi, S. Weiner, *J. Am. Chem. Soc.* **1993**, *115*, 11691–11697.
- [11] C. Cerini, V. Peyrot, C. Garnier, L. Duplan, S. Veessler, J. P. Le Caer, J. P. Bernard, H. Bouteille, R. Michel, A. Vazi, P. Dupuy, B. Michel, Y. Berland, J. M. Verdier, *J. Biol. Chem.* **1999**, *274*, 22266–22274.
- [12] a) A. P. Demchenko, *Topics in Fluorescence Spectroscopy*, Vol. 3 (Ed.: J. R. Lackowicz), Plenum, New York, **1992**, pp. 77; b) L. W. Ruddock, T. R. Hirst, R. B. Freedman, *Biochem. J.* **1996**, *315*, 1001–1005.
- [13] a) F. J. Blanco, G. Rivas, L. Serrano, *Nat. Struct. Biol.* **1994**, *1*, 584–590; b) M. C. Mannin, M. Illangasekare, R. W. Woody, *Biophys. Chem.* **1998**, *31*, 77–86.
- [14] a) G. D. Fasman, *Circular Dichroism and the Conformational Analysis of Biomolecules*, Plenum, New York, **1996**; b) S. C. Shankaramma, S. K. Singh, A. Sathyamurthy, P. Balaram, *J. Am. Chem. Soc.* **1999**, *121*, 5360–5363.
- [15] D. S. Wishart, B. D. Sykes, F. M. Richards, *J. Mol. Biol.* **1991**, *222*, 311–333.
- [16] a) J. S. Evans, *Curr. Opin. Colloid Interface Sci.* **2003**, *8*, 48–54; b) B. A. Wustman, J. C. Weaver, D. E. Morse, J. S. Evans, *Langmuir* **2003**, *19*, 9373–9381.